

Jet-driven active galactic nucleus feedback in galaxy formation before black hole formation

EALEAL BEAR¹ AND NOAM SOKER^{1,2}

¹*Department of Physics, Technion Israel Institute of Technology, Haifa 3200003, Israel*

²*Guangdong Technion Israel Institute of Technology, Guangdong Province, Shantou 515069, China*

ABSTRACT

We propose a scenario where during galaxy formation an active galactic nucleus (AGN) feedback mechanism starts before the formation of a supermassive black hole (SMBH). The supermassive star (SMS) progenitor of the SMBH accretes mass as it grows and launches jets. We simulate the evolution of SMSs and show that the escape velocity from their surface is \approx several $\times 10^3$ km s⁻¹, with large uncertainties. We could not converge with the parameters of the evolutionary numerical code MESA to resolve the uncertainties for SMS evolution. Under the assumption that the jets carry about ten percent of the mass of the SMS, we show that the energy in the jets is a substantial fraction of the binding energy of the gas in the galaxy/bulge. Therefore, the jets that the SMS progenitor of the SMBH launches carry sufficient energy to establish a feedback cycle with the gas in the inner zone of the galaxy/bulge, and hence, set a relation between the total stellar mass and the mass of the SMS. As the SMS collapses to form the SMBH at the center, there is already a relation (correlation) between the newly born SMBH mass and the stellar mass of the galaxy/bulge. During the formation of the SMBH it rapidly accretes mass from the collapsing SMS and launches very energetic jets that might unbind most of the gas in the galaxy/bulge.

Keywords: galaxies: active – (galaxies:) quasars: supermassive black holes – galaxies: jets

1. INTRODUCTION

The formation and evolution of supermassive stars (SMSs) that might collapse to form supermassive black holes (SMBHs) have many open questions (e.g., Omukai, & Palla 2003; Visbal et al. 2014; Sakurai et al. 2015; Luo et al. 2018; Woods et al. 2017; Tagawa et al. 2019; Woods et al. 2019). The basic scenario is that primordial gas clouds contract to form supermassive primordial Pop III stars that grow to masses of about $10^4 - 10^6 M_\odot$ by high accretion rates (e.g., Agarwal et al. 2012; Johnson et al. 2014; Agarwal et al. 2016), and then the SMSs collapse to form BHs that by further accretion grow to SMBHs with masses up to $\approx 10^9 M_\odot$ (e.g., Ardaneh et al. 2018; Umeda et al. 2016). The motivation to study this scenario (e.g., Whalen et al. 2013; Ardaneh et al. 2018; Umeda et al. 2016; Sakurai et al. 2016; Hirschi 2017; Ardaneh et al. 2018; Matsukoba et al. 2019) comes from the difficulties for other theoretical scenarios to form SMBHs, masses of $10^9 M_\odot$, at high redshifts of $z \gtrsim 6$

(for details and references see, e.g., Glover 2016; Smith, & Bromm 2019).

We note that there is a debate whether SMSs can form at all, with some arguments for (e.g., Umeda et al. 2016; for numerical simulations of a collapse to form SMBH see, e.g., Shibata et al. 2016) and some against this scenario (e.g. Dotan, & Shaviv 2012; Yoon et al. 2015; Latif, & Ferrara 2016; Corbett Moran et al. 2018). For example, one of the unsettled issues is whether fragmentation halts the formation process of SMSs (e.g., Bromm et al. 1999; Omukai et al. 2008; Suazo et al. 2019) or not (e.g., Begelman 2010; Corbett Moran et al. 2018; Suazo et al. 2019). The efficiency of fragmentation may (e.g. Hosokawa et al. 2013) or may not (e.g., Corbett Moran et al. 2018) be connected to the metallicity of the parent cloud.

In the present study we adopt the collapsing SMS scenario for the formation of SMBHs, and discuss its implications to the feedback mechanism at early times of galaxy formation. Umeda et al. (2016) argue that SMSs can form and grow by high mass accretion rates into these almost fully convective stars (e.g., Uchida et al. 2017; Johnson et al. 2012). In our study, we assume that the accretion takes place through an accretion disk

that launches jets. Many researchers study jets from massive stars of $M \gtrsim 10M_\odot$ (e.g., Fuller et al. 1986; Garatti 2018; McLeod et al. 2018), but the situation is more complicated and uncertain in SMSs. Latif & Schleicher (2016) study a SMS with a mass of 10^5M_\odot and with a luminosity of 10^6L_\odot that launches jets with a terminal velocity (the velocity at large distances from the star) of $v_j = 1200 \text{ km s}^{-1}$, and argue that the feedback mechanism due to these jets is significant at this early stage of evolution. We adopt the view that SMSs launch jets as they accrete mass at high rates. We will try to estimate the terminal velocities of such jets and their role in the feedback during galaxy formation.

In section 2 we discuss previous calculations and our radii calculations of SMSs. In section 3 we discuss the implications of our finding to very early feedback in galaxy formation. Our short summary is in section 4.

2. SUPERMASSIVE STARS WITH MESA

There are many numerical and physical difficulties in simulating SMSs, $M \gtrsim 10^4M_\odot$, with the stellar evolution code MESA (Modules for Experiments in Stellar Astrophysics, version 10398; Paxton et al. 2011, 2013, 2015, 2018, 2019). Thorough studies of using MESA exist up to stellar masses of $1000M_\odot$ (e.g., Paxton et al. 2011; Smith 2014), but only scarce numerical evolution, mostly with other numerical codes, exist for more massive stars. Due to these difficulties, we limit our study only to some general stellar parameters relevant to our goal of exploring very early feedback in galaxy formation. Namely, we study the radius as function of mass for these SMSs, $M_{\text{SMS}} \simeq 10^4 - 10^6M_\odot$. As well, we limit our study to a metallicity value of $Z = 0$.

Earlier studies using different numerical codes and analytical estimates did not reach full agreement on the radii of SMS. While some derive radii of $R_{\text{SMS}} \simeq 10^4R_\odot$ for SMS of masses of $M_{\text{SMS}} \simeq 10^5M_\odot$ (e.g., Hosokawa et al. 2013; Haemmerlé, & Meynet 2019), other obtained smaller radii, like Surace et al. (2019), which claimed that SMSs are bluer and their typical radii are only about $\text{few} \times 10^3R_\odot$. Some of the differences might result from different conditions. For example, Surace et al. (2019) neglected the effect of radiation pressure on accreted mass, and Hosokawa et al. (2016) included accretion during the evolution. In the simulation by Hosokawa et al. (2013), the stellar radius increases monotonically with the stellar mass as long as the accretion rate stays above $\dot{M} > 10^{-2}M_\odot \text{ yr}^{-1}$ (for more details see their figure 6). Hosokawa et al. (2013) conclude that pulsational mass-loss and stellar UV feedback do not significantly affect the evolution of SMSs that grow by rapid mass accretion rates. As well, Haemmerlé et

al. (2018) find large variations in the radii when they use different accretion rates onto the SMSs.

With these earlier large uncertainties in mind, we turn to describe our MESA numerical results. We describe the setting of MESA in Appendix A. Readers interested only in the results can skip Appendix A and continue with the description below.

We take the common practice in MESA and divide the evolution to pre-main sequence (PMS) and later phases (e.g., Shiode, & Quataert 2014). To minimize the parameter search and fine tuning, when possible, we use the default settings and numerical parameters of MESA, while in other cases we set different parameters that allow us to follow evolution up to core hydrogen depletion. Numerical difficulties dictate the numerical termination time of the evolution to be when the hydrogen in the core is depleted down to $X = 10^{-5}$.

In Fig. 1 we present the stellar radius at the end of the simulation for each of the 25 simulations whose parameters we describe in Appendix A.

We find in our simulations that the radius of a SMS with $M_{\text{SMS}} \gtrsim 5 \times 10^5M_\odot$ fluctuates as the SMS evolves from the main sequence to hydrogen exhaustion, with a typical amplitude of more than 30%. We do not study the sources of these fluctuations (numerical or physical) as this requires a thorough study of the numerical code and a comparison between codes, which is beyond the scope of the present study. We rather take the final value at the termination time.

In Fig. 1 we present the final radius as function of final mass for different runs using MESA (marked by the number of the run). The final mass in our simulations is lower because we include mass-loss. We list the different parameters for each run, including initial and final masses and the stellar age at the end of simulations, in Table 1 in Appendix A.

The orange line on Fig. 1 is from figure 2 of Haemmerlé, & Meynet (2019), and the gray line is from figure 2 of Hosokawa et al. (2013). The blue line is an analytical estimate from Hosokawa et al. (2012). The green line is based on Begelman (2010) who calculates the stellar radius according to

$$R_{\text{SMS}} = 5.8 \times 10^{13} \left(\frac{\dot{M}_{\text{SMS}t}}{10^6M_\odot} \right)^{0.5} \left(\frac{T_c}{10^8 \text{ K}} \right)^{-1} \text{ cm}, \quad (1)$$

where, \dot{M}_{SMS} is the accretion rate at time t , and T_c is the core's temperature. In drawing equation (1) we take $\dot{M}_{\text{SMS}t}$ to be the initial stellar mass and we take T_c from the numerical results of MESA at the end of each simulation.

Hosokawa et al. (2013) study rapidly mass-accreting stars by numerically solving their interior structure with

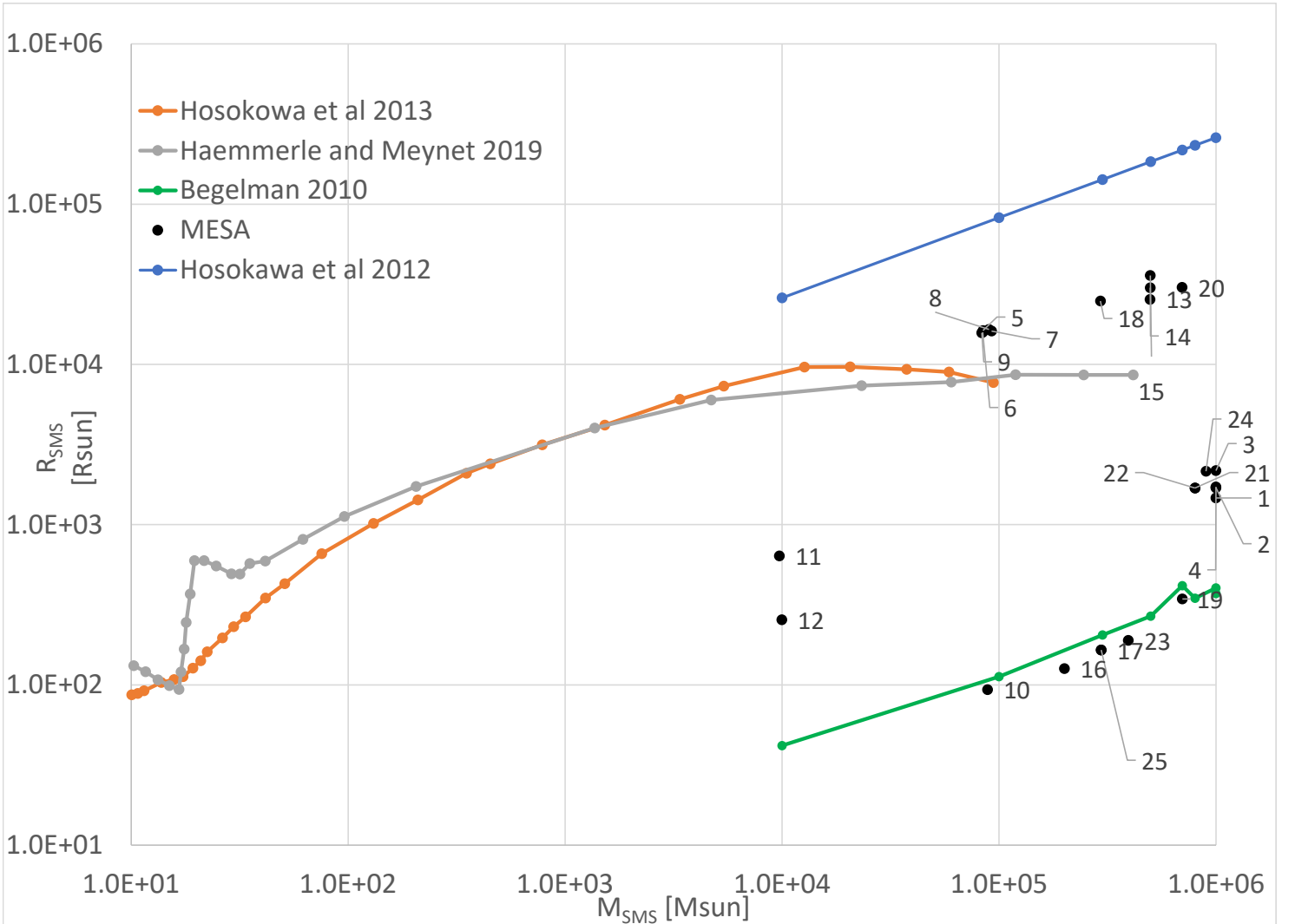


Figure 1. Radius vs. mass. Orange line (and dots) are taken from figure 2 in Haemmerlé, & Meynet (2019). Gray line (and dots) are taken from figure 2 in Hosokawa et al. (2013). Both were taken at what appears to be zero metallicity. The green line is calculated according to Begelman (2010) relationship for such massive stars. The blue line is an analytical estimate from Hosokawa et al. (2012). Black dots depict our MESA calculations for different setups according to Table 1 in Appendix A. We show here only runs that converged, as in many cases the numerical code could not convergence.

an energy output (their figure 2) and without an energy output (their figure 7). The difference between these two options for our range of mass ($\gtrsim 10^4 M_\odot$) is negligible and hence we present in our figure the option of the energy output. Hosokawa et al. (2013) find (orange line in Fig. 1) that the photosphere of SMSs increases with mass up to $R_{\text{SMS}} \simeq 3 \times 10^4 R_\odot$. Beyond this mass, the radius decreases.

Haemmerlé et al. (2018) and Haemmerlé, & Meynet (2019) study the evolution of rotating SMSs up to about masses of $10^5 M_\odot$. Haemmerlé, & Meynet (2019) study

the effect of magnetic coupling between the star and its winds on the angular momentum accreted from a Keplerian disc. They find that magnetic coupling can remove angular momentum excess as accretion to the star proceeds. From their figure 2, we learn that the SMS radius increases with SMS mass up to $M_{\text{SMS}} \simeq 3 \times 10^4 M_\odot$. From Fig. 1 we see that Haemmerlé, & Meynet (2019) and Hosokawa et al. (2013) have similar radius to mass relation.

In addition to the above numerical results, we also draw two analytical approximations on Fig. 1, one (blue

line) by Hosokawa et al. (2012) where the radius is proportional to the square root of the mass, and the other (green line) by Begelman (2010) as given in equation (1). Interestingly, these two lines, more or less delimit the large range of radii we find with MESA, and the two similar lines by Haemmerlé, & Meynet (2019) and Hosokawa et al. (2013).

We conclude that we can simulate SMSs with MESA, but we could not converge on the best numerical parameters to use. The reason we can use our present results despite the large uncertainties is that we need only the gravitational potential well of the SMSs. This determines the velocity of the jets that the accretion disk might launch.

3. THE FEEDBACK MECHANISM: ENERGY AND JETS

There are three phases of feedback from the central object in the scenario we study here. The first one takes place when the SMS grows and launches jets, the second one is a very short phase during which the newly born SMBH launches very powerful jets as it accretes mass at a very high rate from the collapsing SMS, while the third feedback phase might last for up to billions of year (even until present) as the SMBH accretes mass from the interstellar medium. We now examine the first two phases.

3.1. Feedback during SMS growth phase

We expect the SMS to launch jets during its formation, as other young stars do. Namely, the SMS launches jets at the escape velocity and with a mass outflow rate of about $\eta_{\text{SMS},j} \approx 0.1$ of the accretion rate. From Fig. 1 we find the escape velocity for $M_{\text{SMS}} \gtrsim 10^4 M_\odot$ to be $v_j = v_{\text{esc}} \simeq 6000 \text{ km s}^{-1} (M_{\text{SMS}}/10^6 M_\odot)^{1/2}$. The total energy the jets carry is then

$$E_{\text{SMS},j} = \int_0^{M_c} \frac{1}{2} v_j^2 \eta_{\text{SMS},j} dM \simeq 9 \times 10^{11} \times \left(\frac{\eta_{\text{SMS},j}}{0.1} \right) \left(\frac{M_c}{10^6 M_\odot} \right)^2 M_\odot \text{ km}^2 \text{ s}^{-2} \quad (2)$$

where M_c is the SMS mass when it starts collapsing, and $9 \times 10^{11} M_\odot \text{ km}^2 \text{ s}^{-2} = 1.8 \times 10^{55} \text{ erg}$.

Let us consider the gas in the bulge of such a new galaxy. The velocity dispersion of host bulges of SMBHs with masses of $M_{\text{BH}} \simeq 10^6 M_\odot$ is $\sigma_e \simeq 60 \text{ km s}^{-1}$ (e.g., Gebhardt et al. 2000; de Nicola et al. 2019). As well, the stellar bulge mass is $M_{\text{bulge}} \approx 10^3 M_{\text{BH}}$ (e.g., Schutte et al. 2019), where by bulge we refer to the spherical (more or less) component of the galaxy, which might be the entire stellar mass in elliptical galaxies. We assume

a similar gas mass at the early phase of galaxy formation. The approximate total virial energy of the gas is therefore $E_{\text{bulge,gas}} \approx M_{\text{bulge}} \sigma_e^2$, which amounts to

$$E_{\text{bulge,gas}} \approx 3.6 \times 10^{12} \left(\frac{M_c}{10^6 M_\odot} \right) M_\odot \text{ km}^2 \text{ s}^{-2}. \quad (3)$$

The conclusion from equations (2) and (3) is that the energy in the jets during the SMS growth is non-negligible. This is particularly the case if we consider that the jets interact only with the polar gas they encounter along their propagation direction. For a half opening angle of $\alpha_j \lesssim 40^\circ$ the energy in the jets is larger than the gas energy, so the jets can substantially heat and/or unbind some of the gas. If the SMS radius is $\approx 10^3 R_\odot$ instead of $\approx 10^4 R_\odot$, then the jets carry about ten times more energy and the feedback with the galaxy formation is much more important during this phase.

The life time of a SMS with a mass of $\approx 10^6 M_\odot$ and a radius of $\approx 10^4 R_\odot$ is $t_{\text{SMS}} \approx 10^6 \text{ yr}$ (see Appendix A). During that time the jets can reach a distance of $R_{\text{FB}} \approx 6 \text{ kpc}$, where we take the jet velocity as above. This is much larger than the size of a bulge hosting such a SMBH. The region from which gas can feed the SMS is much smaller. Taking the velocity for the inflow to be as the velocity dispersion, the feeding zone has a radius of $R_{\text{feed}} \approx \sigma_e t_{\text{SMS}} \approx 0.06 \text{ kpc}$. This radius is about one tenth of the size of the bulge. This is like the situation in cooling flows in clusters of galaxies, where the hot gas extends to hundreds of kpc, while the gas with a cooling time shorter than the age of the galaxy resides in a region that is only about one tenth of that radius. Namely, the region where feedback takes place is much smaller than the total extends of the gas. It is quite possible that during the very early time of galaxy formation there is a small scale cooling flow (Soker 2010). Here, we strengthen the preliminary idea of Soker (2016) that the feedback with the inner region of the interstellar gas starts during the growth phase of the SMS.

3.2. Outcomes of SMBH formation

Earlier studies examined the process where the newly born SMBH launches jets as it accretes mass from the collapsing SMS (e.g., Matsumoto et al. 2016; Uchida et al. 2017), and the feedback with the environment that the jets might induce (e.g., Matsumoto et al. 2015). Matsumoto et al. (2015) and Matsumoto et al. (2016) who discussed gamma ray bursts from these jets took the jet energy to be $E_{\text{BH},j} = \eta_{\text{BH},j} M_c c^2 \approx 10^{55-56} \text{ erg}$ with $\eta_{\text{BH},j} = 6.2 \times 10^{-4}$, and where M_c is the collapsing mass. Matsumoto et al. (2015) estimated the event rate to be about one per year. We note that the $M_c = 10^5 M_\odot$ SMS model of Matsumoto et al. (2015) has a radius of about

$10^3 R_\odot$, about one order of magnitude smaller than what we use here. Using a smaller radius would imply much higher jets' velocity and therefore a much more efficient feedback during the growth phase of the SMS. These papers, among others, derive many properties, like gamma ray bursts, that we do not consider here. Our only goal is to argue that AGN feedback during galaxy formation has started before the formation of the SMBH. In section 4 we will discuss the implications of this very early feedback process.

Let us derive the basic parameters of the jets for the case we study here, and mention their relevance to the present study. The accretion phase will last for about the free fall time of the outer region of the SMS. This time is $\tau_{\text{ff}} = 0.056(R/10^4 R_\odot)^{3/2}(M_c/10^6 M_\odot)^{-1/2}$ yr. Sun et al. (2017) conduct magnetohydrodynamic simulations of a collapsing SMS and estimate the accretion torus lifetime to be $t \approx 0.003(M_c/10^6)$ s, which is shorter than the free fall time we take here, or about the same if the radius of the SMS is about $10^3 R_\odot$ and not about $10^4 R_\odot$. This very short accretion phase implies that there is no time to establish a feedback cycle with the interstellar medium. As the paper cited above already noticed, we have here an explosion, more similar to low mass long gamma ray bursts.

However, the total energy in the jets is very large

$$E_{\text{BH,j}} = \eta_{\text{BH,j}} M_c c^2 = 9 \times 10^{13} \times \left(\frac{\eta_{\text{BH,j}}}{0.001} \right) \left(\frac{M_c}{10^6 M_\odot} \right) M_\odot \text{ km}^2 \text{ s}^{-2}. \quad (4)$$

This energy, of $E_{\text{BH,j}} = 2 \times 10^{57}$ erg for the above scaling, can be more than an order of magnitude larger than the binding energy of the gas in the bulge hosting the newly born SMBH (eq. 3). As Matsumoto et al. (2015) already discussed, these jets can expel all the gas from the young low-mass galaxy (or bulge). This leaves the galactic stellar mass to be that of the mass of the stars that have been already formed, and the SMBH mass to be about equal to that of the SMS. Namely, the feedback during the SMS growth phase determines the relation between the bulge and SMBH masses. We discuss this further in section 4.

4. DISCUSSION AND SUMMARY

The goal of the present study is to strengthen the case for a very early feedback process between the growth of the total stellar population mass of a bulge (or a galaxy) and the growth of its central massive body. The motivation to consider a very early feedback comes from the correlation between the mass of the SMBH and the properties of its host galaxy (bulge; e.g., Benedetto et al. 2013; Graham, & Scott 2013; Saxton et al. 2014), in

particular the total stellar mass. The properties of the bulge-SMBH masses correlation itself shows that this correlation cannot be driven by many mergers of low mass galaxies (Ginat et al. 2016). This hints that there is a very early process, most likely a feedback process, that starts to establish the correlation.

We therefore examine the possibility that jets from SMS progenitors of SMBHs have enough energy to start a feedback process even before a SMBH is formed. The jets that these SMSs launch are non-relativistic, but rather have a velocity of $v_j \simeq \text{several} \times 1000 \text{ km s}^{-1}$ (section 3.1). This is not a problem as observations show that even in evolved (old) AGN non-relativistic outflows of similar velocities can drive a feedback process (e.g., Chamberlain et al. 2015; Xu et al. 2019).

We summarize our main results first, and then their implications.

(1) We could not resolve the question of whether SMSs of $\approx 10^6 M_\odot$ have a radius of $R \approx 10^3 R_\odot$ or $R \approx 10^4 R_\odot$. We therefore adopted the results of Haemmerlé, & Meynet (2019) and Hosokawa et al. (2013) and took $R \approx 10^4 R_\odot$ (see recent review by Hosokawa 2018). To resolve this question, there is a need for a thorough and detailed study with MESA. These SMSs live for $t_{\text{SMS}} \approx 10^6$ yr.

(2) Under this assumption and the assumptions that the SMSs launch jets at the escape velocity from its surface and that about ten percent of the accreted mass is carried out by the jets, the total kinetic energy of the jets is $E_{\text{SMSs,j}} \approx \text{few} \times 10^{55} \text{ erg} \simeq 10^{12} M_\odot \text{ km}^2 \text{ s}^{-2}$ (equation 2). This might be a substantial fraction of the energy of the gas in interstellar medium under the assumption that the gas mass is $M_{\text{bulge}} \approx 10^3 M_{\text{BH}}$ (equation 3).

(3) As we discussed in section 3.1, during the SMS growth phase that lasts for about 10^6 yr (e.g., Hosokawa et al. 2013 and Table 1 in Appendix A), the jets can propagate through the bulge (or small new galaxy), and the jets might establish a feedback with the interstellar medium within about 0.05 kpc. A situation similar to that in cooling flows in clusters of galaxies might take place here, but within a much smaller region (Soker 2010).

(4) As the SMS collapsing to form a SMBH, the SMBH accretes mass at a very high rate from the collapsing SMS and is likely to launch jets. As earlier studies concluded, e.g., Matsumoto et al. (2015), the energy in these jets (equation 4) might be much larger than the binding energy of the interstellar such that the jets expel most or all of this gas. Klammer et al. (2004), on the other hand, discuss jet-induced star formation scenario from

observation and noted its implication to galaxy formation.

One of the conclusions from our findings is that even in systems where the accretion of gas onto the bulge and the accretion of mass onto the SMBH are negligible after SMBH formation, the correlation between the SMBH mass and total stellar bulge (or dwarf galaxy) mass has been already established at earlier times. Namely, this correlation holds even in the least massive systems.

Yang et al. (2019), for example, argue that the correlated growth of the masses of the bulge and of the SMBH it hosts started very early in the Universe, at a redshift of $z = 3$ or earlier even. We suggest that this correlated growth started with the formation of the SMS progenitor of the SMBH.

This research was supported by a grant from the Israel Science Foundation.

REFERENCES

- Agarwal, B., Khochfar, S., Johnson, J. L., Neistein, E., Dalla Vecchia, C. and Livio, M. 2012, *MNRAS*, 425, 2854
- Agarwal, B., Smith, B., Glover, S., Natarajan, P., & Khochfar, S. 2016, *MNRAS*, 459, 4209
- Ardaneh, K., Luo, Y., Shlosman, I., Nagamine, K., Wise, J. H. and Begelman, M. C. 2018, *MNRAS*, 479, 2277.
- Begelman, M. C. 2010, *MNRAS*, 402, 673.
- Benedetto, E., Fallarino, M. T., & Feoli, A. 2013, *A&A*, 558, A108
- Bromm, V., Coppi, P. S., & Larson, R. B. 1999, *ApJ*, 527, L5.
- Chamberlain, C., Arav, N., & Benn, C. 2015, *MNRAS*, 450, 1085
- Corbett Moran, C., Grudić, M. Y., & Hopkins, P. F. 2018, *ArXiv e-prints* , arXiv:1803.06430.
- Cox, J. P., & Giuli, R. T. 1968, *Principles of stellar structure*.
- de Nicola, S., Marconi, A., & Longo, G. 2019, *MNRAS*, 2130
- Dotan, C., & Shaviv, N. J. 2012, *MNRAS*, 427, 3071
- Fuller, J., Cantiello, M., Lecoanet, D., & Quataert, E. 2015, *ApJ*, 810, 101
- Garatti, A. C. o 2018, arXiv:1807.09539
- Gebhardt, K., Bender, R., Bower, G., et al. 2000, *ApJL*, 539, L13
- Gilkis, A. 2018, *MNRAS*, 474, 2419.
- Ginat, Y. B., Meiron, Y., & Soker, N. 2016, *MNRAS*, 461, 3533
- Glover, S. C. O. 2016, *ArXiv e-prints* , arXiv:1610.05679.
- Gofman, R. A., Gilkis, A., & Soker, N. 2018, *MNRAS*, 478, 703.
- Graham, A. W., & Scott, N. 2013, *ApJ*, 764, 151
- Fuller, G. M., Woosley, S. E., & Weaver, T. A. 1986, *ApJ*, 307, 675
- Haemmerlé, L., & Meynet, G. 2019, *A&A*, 623, L7
- Haemmerlé, L., Woods, T. E., Klessen, R. S., et al. 2018, *MNRAS*, 474, 2757
- Heger, A., Langer, N., & Woosley, S. E. 2000, *ApJ*, 528, 368.
- Heger, A., Woosley, S. E., & Spruit, H. C. 2005, *ApJ*, 626, 350.
- Henry, L., Vardya, M. S., & Bodenheimer, P. 1965, *ApJ*, 142, 841.
- Hirschi, R. 2017, *Handbook of Supernovae*, 567.
- Hosokawa, T. 2018, *arXiv e-prints* , arXiv:1807.06355.
- Hosokawa, T., Hirano, S., Kuiper, R., et al. 2016, *ApJ*, 824, 119.
- Hosokawa, T., Omukai, K., & Yorke, H. W. 2012, *ApJ*, 756, 93
- Hosokawa, T., Yorke, H. W., Inayoshi, K., Omukai, K., & Yoshida, N. 2013, *ApJ*, 778, 178
- Johnson, J. L., Agarwal, B., Whalen, D. J., et al. 2012, *American Institute of Physics Conference Series*, 313.
- Johnson, J. L., Whalen, D. J., Agarwal, B., Paardekooper, J.-P., & Khochfar, S. 2014, *MNRAS*, 445, 686
- Keszthelyi, Z., Wade, G. A., & Petit, V. 2017, *The Lives and Death-throes of Massive Stars*, 250
- Kippenhahn, R., Ruschenplatt, G., & Thomas, H.-C. 1980, *A&A*, 91, 175.
- Klamer, I. J., Ekers, R. D., Sadler, E. M., et al. 2004, *ApJL*, 612, L97
- Latif, M. A., & Ferrara, A. 2016, *Publications of the Astronomical Society of Australia*, 33, e051.
- Latif, M. A., & Schleicher, D. R. G. 2016, *A&A*, 585, A151
- Luo, Y., Ardaneh, K., Shlosman, I., et al. 2018, *MNRAS*, 476, 3523
- Matsukoba, R., Takahashi, S. Z., Sugimura, K., et al. 2019, *MNRAS*, 484, 2605.
- Matsumoto, T., Nakauchi, D., Ioka, K., Heger, A., & Nakamura, T. 2015, *ApJ*, 810, 64
- Matsumoto, T., Nakauchi, D., Ioka, K., & Nakamura, T. 2016, *ApJ*, 823, 83
- McLeod, A. F., Reiter, M., Kuiper, R., Klaassen, P. D., & Evans, C. J. 2018, *Nature*, 554, 334
- Omukai, K., & Palla, F. 2003, *ApJ*, 589, 677.

- Omukai, K., Schneider, R., & Haiman, Z. 2008, *ApJ*, 686, 801
- Paxton, B., Bildsten, L., Dotter, A., Herwig, F., Lesaffre, P. and Timmes, F. 2011, *ApJS*, 192, 3
- Paxton, B., Cantiello, M., Arras, P., et al. 2013, *ApJS*, 208, 4
- Paxton, B., Marchant, P., Schwab, J., et al. 2015, *ApJS*, 220, 15
- Paxton, B., Schwab, J., Bauer, E. B., et al. 2018, *The Astrophysical Journal Supplement Series*, 234, 34.
- Paxton, B., Smolec, R., Schwab, J., et al. 2019, *ApJS*, 243, 10, arXiv:1903.01426
- Rogers, F. J., & Nayfonov, A. 2002, *ApJ*, 576, 1064.
- Sakurai, Y., Hosokawa, T., Yoshida, N., et al. 2015, *MNRAS*, 452, 755.
- Sakurai, Y., Vorobyov, E. I., Hosokawa, T., et al. 2016, *MNRAS*, 459, 1137.
- Saxton, C. J., Soria, R., & Wu, K. 2014, *MNRAS*, 445, 3415
- Schutte, Z., Reines, A., & Greene, J. 2019, arXiv e-prints, arXiv:1908.00020
- Shibata, M., Sekiguchi, Y., Uchida, H. and Umeda, H. 2016, *PhRvD*, 94, 21501, arXiv: 1606.07147
- Shiode, J. H. 2013, Ph.D. Thesis.
- Shiode, J. H., & Quataert, E. 2014, *ApJ*, 780, 96.
- Smith, N. 2014, *ARA&A*, 52, 487
- Smith, A., & Bromm, V. 2019, arXiv e-prints, arXiv:1904.12890
- Soker, N. 2010, *MNRAS*, 407, 2355
- Soker, N. 2016, *NewAR*, 75, 1
- Suazo, M., Prieto, J., & Escala, A. 2019, *Boletin de la Asociacion Argentina de Astronomia La Plata Argentina*, 61, 192; arXiv:1903.03637
- Surace, M., Zackrisson, E., Whalen, D. J., et al. 2019, *MNRAS*, 488, 3995; arXiv:1904.01507
- Sun, L., Paschalidis, V., Ruiz, M. and Shapiro, S, L. 2017, *PhRvD*, 96, 43006.
- Timmes, F. X., & Swesty, F. D. 2000, *The Astrophysical Journal Supplement Series*, 126, 501.
- Tagawa, H., Haiman, Z., & Kocsis, B. 2019, arXiv e-prints, arXiv:1909.10517
- Uchida, H., Shibata, M., Yoshida, T., Sekiguchi, Y., & Umeda, H. 2017, *PhRvD*, 96, 083016
- Umeda, H., Hosokawa, T., Omukai, K. and Yoshida, N. 2016, *ApJ*, 830, L34.
- Visbal, E., Haiman, Z., & Bryan, G. L. 2014, *MNRAS*, 445, 1056
- Whalen, D. J., Even, W., Smidt, J., et al. 2013, *ApJ*, 778, 17.
- Woods, T. E., Agarwal, B., Bromm, V., et al. 2019, *PASA*, 36, e027; arXiv:1810.12310
- Woods T. E., Heger A., Whalen D. J., Haemmerlé L., Klessen R. S., 2017, *ApJL*, 842, L6
- Xu X., Arav N., Miller T., Benn C., 2019, *ApJ*, 876, 105
- Yang G., Brandt W. N., Alexander D. M., Chen C.-T. J., Ni Q., Vito F., Zhu F.-F., 2019, *MNRAS*, 485, 3721
- Yoon, S.-C., Kang, J., & Kozyreva, A. 2015, *ApJ*, 802, 16

APPENDIX

A. NUMERICAL SETUP

This appendix contains technical description of the relevant physical and numerical parameters of the numerical code MESA. Parameters not addressed here are as in the 'controls' and 'star jobs' default inlists of MESA.

We could not achieve convergence of SMS models with the default MESA parameters (both regular and those adopted for high mass). Therefore, we changed a few parameters from different categories as follows.

A.1. *Instabilities*

To deal with stellar instability we changed a set of parameters that includes the following. The shear instability parameter D_DSI , the Solberg-Hoiland parameter D_SH , the secular shear instability D_SSI , the Eddington-Sweet circulation parameter D_ES , the Goldreich-Schubert-Fricke D_GSF parameter, and the Spruit-Tayler dynamo parameter D_ST (for more details see Heger et al. 2000, 2005). At default settings, all these instability parameters in MESA are set to 0. Two other parameters: $am_D_mix_factor$ and $am_nu_visc_factor$ (which are part of the algebraic formula that MESA uses to calculate the diffusion coefficient for mixing of material) are 0 and 1 in the default setting, respectively.

We checked the impact of these instability parameters according to Shiode, & Quataert (2014) and Gilkis (2018). Shiode, & Quataert (2014) studied massive stars of $M > 30M_\odot$ and took $D_SSI_factor = D_ES_factor = D_GSF_factor = 1.16$, keeping all other parameters at their default values. Gilkis (2018) set the parameters at: $am_nu_visc_factor = 0$, $am_D_mix_factor = \frac{1}{30}$ (Heger et al. 2000), and $D_DSI_factor = D_SH_factor = D_SSI_factor = D_ES_factor = D_GSF_factor = 1$. We also take $D_ST_factor = 1$.

In our simulations we adopt one of three options. (A) Instability parameters according to Gilkis (2018) and $D_ST_factor = 1$, (B) instability parameters according to the MESA default values, and (C) instability parameters according to Shiode, & Quataert (2014). We list the parameters, both instability parameters and others, of 25 of our simulations in Table 1. In many other simulations MESA did not converge and we do not present these cases here.

A.2. *Structure parameters*

We activated two parameters (*include_dmu_dt_in_eps_grav* and *fix_eps_grav_transition_to_grid*) that are deactivated in the default setting. The parameter *include_dmu_dt_in_eps_grav* includes the contribution from composition changes when activated. We activated this parameter in many of our simulations as recommended for high temperature in MESA. The purpose of *fix_eps_grav_transition_to_grid* is to fix the transition region of the mesh and it helps with convergence near the Eddington limit. In several runs we activated this parameter (as in some of the simulation of Paxton et al. (2018); their Figs 49 - 51). We note that run 22 was done twice. Once as noted in the table and the second time when *use_ODE_var_eqn_pairing* is activated (default setting is deactivated). The final radius and age were identical.

A.3. *Mixing parameters*

The parameter *okay_to_reduce_gradT_excess* adjusts the gradient of the temperature to boost efficiency of energy transport. We activated this parameter (in the default setting it is deactivated). We note that Keszthelyi et al. (2017) also activated it for a stars of $15M_\odot$.

A.4. *Mixing length theory (MLT)*

We checked two settings for the *MLT option*, Cox (Cox, & Giuli 1968) which is the default setting and Henyey (Henyey et al. 1965). The Henyey setting allows the convective efficiency to vary with the opaqueness of the convective element. Near the outer layers of stars, this is an important effect for convective zones, while the Cox setting assumes high optical depths and no radiative losses (for more details see Paxton et al. 2011). We achieved convergence for several combinations as indicated in Table 1.

A.5. *Non-default parameters identical to all runs*

Below we list parameters that we changed from their default values in the same manner in all runs.

- Opacity. We used the default setting for the opacity tables (*kappa_file_prefix = 'gs98'*). We activated *use_Type2_opacities* and took 'Zbase' to be identical to the metallicity which we set at 0.

RUN	M_i	M_f	R_f	Age	Instabilities			MLT option			EOS		Max model
	$[M_\odot]$	$[M_\odot]$	$[R_\odot]$	[yr]	A	B	C	I	II	III	a	b	
1	1.00E+06	1.00E+06	1.47E+03	9.34E+04	V			V				V	1d5
2	1.00E+06	1.00E+06	1.70E+03	1.49E+05	V				V			V	!
3	1.00E+06	1.00E+06	2.17E+03	2.35E+05		V		V				V	!
4	1.00E+06	1.00E+06	1.72E+03	2.21E+05	V			V			V	V	1d5
24	9.00E+05	8.99E+05	2.15E+03	3.35E+05	V			V			V	V	5d5
21	8.00E+05	8.00E+05	1.69E+03	1.58E+05	V			V			V	V	1d5
22	8.00E+05	8.00E+05	1.69E+03	1.58E+05	V			V			V	V	5d5
19	7.00E+05	7.00E+05	3.44E+02	3.07E+04	V			V		V		V	1d5
20	7.00E+05	6.98E+05	3.03E+04	1.19E+06	V			V				V	1d5
13	5.00E+05	4.97E+05	2.54E+04	1.58E+06	V				V			V	1d5
14	5.00E+05	4.98E+05	3.01E+04	1.21E+06	V			V			V	V	1d5
15	5.00E+05	4.98E+05	3.59E+04	1.03E+06		V		V			V	V	1d5
23	4.00E+05	3.94E+05	1.89E+02	4.41E+04	V			V		V		V	5d5
25	3.00E+05	2.96E+05	1.65E+02	4.85E+04	V			V		V		V	1d5
17	3.00E+05	2.96E+05	1.65E+02	4.85E+04	V			V		V		V	!
18	3.00E+05	2.93E+05	2.48E+04	1.61E+06	V			V			V	V	5d5
16	2.00E+05	2.00E+05	1.27E+02	5.69E+04	V			V		V		V	!
5	1.00E+05	8.43E+04	1.63E+04	1.58E+06	V				V			V	!
6	1.00E+05	8.41E+04	1.59E+04	1.58E+06	V			V			V	V	!
7	1.00E+05	9.24E+04	1.61E+04	1.55E+06			V	V				V	!
8	1.00E+05	8.99E+04	1.65E+04	1.57E+06		V		V				V	!
9	1.00E+05	8.33E+04	1.57E+04	1.58E+06	V			V				V	!
10	1.00E+05	8.86E+04	9.35E+01	7.80E+04	V					V		V	!
11	1.00E+04	9.72E+03	6.38E+02	1.54E+06	V			V				V	!
12	1.00E+04	9.98E+03	2.55E+02	1.52E+06		V		V				V	!

Table 1. The stellar evolution simulations that converged, i.e., could reach the time of core hydrogen depletion, by descending initial mass. All are marked on Fig. 1. The first five columns give the run number, the initial mass M_i , the final mass M_f which is somewhat lower due to a wind, the final stellar radius R_f , and the age at the termination of the calculation. The other columns list the MESA parameters as we describe in the text. The first group of three columns refers to the instabilities options (section A.1), A: as in Gilkis (2018) and $D_{ST}factor = 1$, (B) According to the MESA default values, and (C) according to Shiode, & Quataert (2014). The first two MLT columns are (I) Henyey for PMS and Cox for main sequence and later, (II) Henyey for both PMS and later evolution (section A.4). The last option (III) allows the code to boost efficiency of energy transport (MESA parameter, *okay_to_reduce_gradT_excess*). In the EOS columns ‘a’ and ‘b’ represent activating the options *Include_dmu_in_eps_grav* and *fix_eps_grav_transition_to_grid*, respectively (for details see MESA defaults). The last column: Max model, limits the number of models in the code. The mark ‘!’ in the last column of Table 1 means that we set no limit on the number of models, i.e., we worked with the default options.

- Mixing parameters. The parameter *mixing_length_alpha* times a local pressure scale height is the mixing length. The default of MESA is *mixing_length_alpha* = 2. For all of the simulations presented in Table 1 we used *mixing_length_alpha* = 1.5 (Shiode, & Quataert 2014; Fuller et al. 2015). The parameter *alpha_semiconvection* which determines efficiency of semiconvective mixing is taken as 1 (default is 0). We took *num_cells_for_smooth_gradL_composition_term* and *threshold_for_gradL_composition_term* as 10 and 0.02, respectively, to help with convergence. The parameter *use_Ledoux_criterion* was activated since thermohaline mixing and semiconvection only applies when *use_Ledoux_criterion* is activated. Regarding the thermohaline coefficients, we used the Kippenhahn method (default option of MESA) for the *thermohaline_option* parameter, while for the *thermohaline_coeff* parameter which determines efficiency of thermohaline mixing we took 1 (the default in MESA is 0).

- Rotation. We checked rotation for fast rotators. We take the angular velocity Ω as $0.3\Omega_c$ where Ω_c is the critical angular velocity, $\Omega_c = \sqrt{\left(1 - \frac{L}{L_{Edd}}\right) \frac{GM}{R^3}}$, L, M and R are the luminosity, total mass and photospheric radius of the star, respectively, and L_{Edd} is the Eddington luminosity (for more details and relevant references see Paxton et al. 2013; Gofman et al. 2018). For slow rotating SMSs we were not able to achieve convergence at these high mass stars, however not all set of parameters were tried.
- Atmosphere. We set the atmosphere as the default option of MESA *simple_atmosphere*. However, we increased the *Pextra_factor* (which is the parameter in-charge for extra pressure in surface boundary conditions) to be 2, to help with convergence (as the manual of MESA recommends).
- Mass-change. We take the default prescriptions of mass-loss. These parameters were changed from the defaults settings to *hot_wind_full_on_T* = 1, *cool_wind_full_on_T* = 0 and *Dutch_scaling_factor* = 1.0. From different runs we conducted and existing examples found in MESA, it is our understanding that MESA does not allow high accretion rates for such massive stars, and hence we do not include accretion. We made small changes to the three parameters of *max_logT_for_k_below_const_q*, *max_logT_for_k_const_mass*, and *min_q_for_k_const_mass*, from their default values of 1, 1 and 0.99 to the values of 0.99, 0.98 and 0.98, respectively.
- Time-step controls. We set the minimum time-step to be *min_timestep_limit* = 10^{-12} s, and took *varcontrol_target* = 10^{-5} . The *varcontrol_target* parameter is the target value for relative variation in the structure from one model to the next.
- Stopping condition. For the pre-main sequence (PMS) phase we used the routine of Shiode (2013) and Shiode, & Quataert (2014). We stop our post-main sequence stellar evolution when the central mass fraction of hydrogen (^1H) drops below 10^{-5} .

In order to limit the total time of the run we chose on several runs to limit *max_model_number* as indicated in the table for each run. The mark ‘!’ in the last column of Table 1 means that we set no limit on the number of models, i.e., we worked with the default options. As can be seen from comparing the final radius of runs 25 with 17, or 21 with 22, the limit on this parameter does not affect much the final result.

- Mesh adjustment. The mesh coefficients were kept according to MESA defaults, except for *max_allowed_nz* that was changed throughout all of our runs to 10^5 .